34th Annual International Conference of the IEEE EMBS
San Diego, California USA, 28 August - 1 September, 2012

Advanced Characterization of Microscopic Kidney Biopsies Utilizing Image Analysis Techniques

Theodosios Goudas , *student Member, IEEE*, Charalampos Doukas, *student Member, IEEE*, Aristotle Chatziioannou *Member, IEEE and* Ilias Maglogiannis, *Senior Member IEEE*

***Abstract*—Correct annotation and identification of salient regions in Kidney biopsy images can provide an estimation of pathogenesis in obstructive nephropathy. This paper presents a tool for the automatic or manual segmentation of such regions along with methodology for their characterization in terms of the exhibited pathology. The proposed implementation is based on custom code written in Java and the utilization of open source tools (i.e. RapidMiner, ImageJ). The corresponding implementation details along with the initial evaluation of the proposed integrated system are also presented in the paper.**

I. INTRODUCTION

The kidney is a multicellular, heterogeneous, multi-structural organ that is responsible for a part of the complex process of blood's purification. As blood flows through the kidneys, waste materials, chemicals and unneeded water are removed out of the body as urine. Kidneys are being affected by many chronic diseases often leading to a slow deterioration of this organ, which implies to an inappropriate cleaning of the blood. Obstructive Nephropathy [1] is the main cause of renal failure, which occurs in all ages but is often met in children and infants. It is caused by obstruction of the urinary tract, with hydronephrosis (which is dilation of the renal pelvis and calyses resulting from obstruction to flow of urine), slowing of the glomerular filtration rate and tubular abnormalities.

Considering that obstructive nephropathy is not a rare disease [1], automated detection of the pathogenic areas on a kidney biopsy image is very useful for the proper assessment of the disease. In this context we have developed a computer-based application, which is able to recognize salient objects (i.e. see in Fig.1 non-Pathogenic Glomerulus, Pathogenic Glomerulus, non-Pathogenic Tubulus and Pathogenic Tubulus) among other regions, aiming at the quantification of the depicted in the image disease. This work is an evolution of [21]. In this paper we present the details of the implemented application along with an initial evaluation.

Ilias Maglogiannis and Theodosios Goudas are with the University of Central Greece, Dep. of Computer Science and Biomedical Informatics (e-mail: imaglo@ucg.gr; goudas@ucg.gr).

Charalampos Doukas is with the University of the Aegean, Dep. of Information & Communication Systems Engineering, Samos, Greece (email: doukas@aegean.gr).

Aristotle Chatziioannou is with the National Hellenic Research Foundation, Institute of Biological Research and Biotechnology, (e-mail: achatzi@eie.gr).

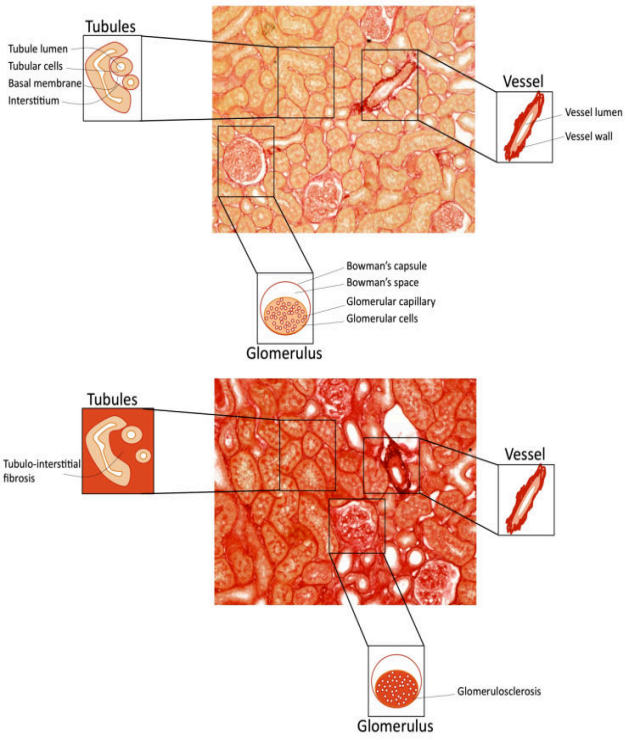

Figure 1. Regions of Interest and their characterization on a kidney biopsy image.

The rest of the paper is organized as follows: Section 2 discusses related work in the field, while Section 3 describes the proposed methodology. Section 4 provides the evaluation results and finally Section 5 concludes the paper.

II. RELATED WORK

The field of microscopy image analysis has occupied several research teams and significant research work may be found in literature in this field. Maglogiannis et al. in [2] present a tool, which classifies biological microscopic images of lung tissue sections with idiopathic pulmonary fibrosis. Similar tools have also been proposed for the assessment of liver fibrosis [3]-[6], the study of micro vascular circulating leukocytes [7], the assessment of testicular interstitial fibrosis, [8], [[9]], or that of lung fibrosis [10]. The use of pattern recognition or classification methods like Support Vector Machines or Neural Networks could enable the design of decision-making algorithms, appropriate to microscopic data. Within this context, a method for evaluation of electron microscopic images of serial sections based on the Gabor

wavelets and the construction of a mapping between the "model" and the "target" image has been proposed in [11]. There are additional research works that could be referred, but to our best knowledge there is no other related work in the literature addressing automated characterization of obstructive nephropathy images.

III. Materials And Methods

An overview of the designed and implemented image processing pipeline is depicted in Fig. 2. The image is divided in blocks (squares) and each block is allocated through a classification procedure to a specific salient object or background. Then a morphological operator based on majority voting is utilized, in order to remove erroneously classified segments of the image.

A. Image Dataset

The utilized image dataset has been obtained from healthy and pathogenic kidney biopsies. In the context of our study, 60 images were utilized, 30 control and 30 pathological. Samples are stained with the Sirius Red technique, which is one of the best-understood techniques of collagen histo-chemistry. In bright-field microscopy collagen are red on a pale yellow, while nuclei are ideally black but may often be grey or brown. In the examined kidney images the pathological findings are connected with alterations in the imaging of the 2 major salient objects: Tubulus and Glomerulus.

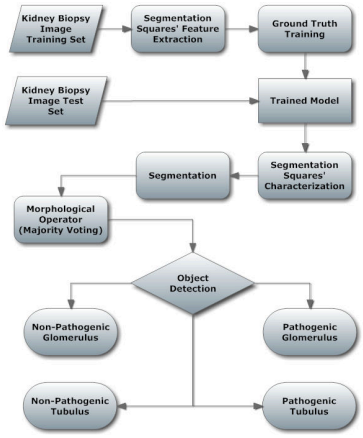

Figure 2. Flow Diagram of the proposed application for the recognition of salient objects in Kidney Biopsy Images

A Nikon Eclipse E400 microscope was used with a Nikon lens Plan Fluor 20x / 0.50; DIC M; ∝ / 0.17 WD 2.1 combined with a Microfire by Optronics camera with the following settings in order to capture the kidney biopsy images. Settings: exposure were as following: 10ms; Red: 105; Green: 100; Blue: 100; Gain: 1; Luminosity: 50; Contrast: 60.

TABLE I. RESULTS OF THE CLASSIFICATION MODELS OF SEGMENTATION WINDOW 37X37

Classifiers		true non-Pathogenic Glomerulus	true non-Pathogenic Tubulus	true Pathogenic Glomerulus	true Pathogenic Tubulus	class precision	Total Accuracy
SVM	pred. non-Pathogenic Glomerulus	381	1	12	12	93.842	
	pred. non-Pathogenic Tubulus	4	244	0	0	98.387	
	pred. Pathogenic Glomerulus	8	0	312	12	93.976	
	pred. Pathogenic Tubulus	4	3	14	314	93.731	
	class recall	**95.970**	**98.387**	**92.308**	**92.899**		**94.701**
KNN	pred. non-Pathogenic Glomerulus	371	7	12	16	91.379	
	pred. non-Pathogenic Tubulus	6	232	0	5	95.473	
	pred. Pathogenic Glomerulus	11	0	311	17	91.740	
	pred. Pathogenic Tubulus	9	9	15	300	90.090	
	class recall	**93.451**	**93.548**	**92.012**	**88.757**		**91.900**
Decision Trees	pred. non-Pathogenic Glomerulus	374	2	13	20	91.443	
	pred. non-Pathogenic Tubulus	4	244	0	4	96.825	
	pred. Pathogenic Glomerulus	11	0	315	11	93.472	
	pred. Pathogenic Tubulus	8	2	10	303	93.808	
	class recall	**94.207**	**98.387**	**93.195**	**89.645**		**93.565**
Naïve Bayes	pred. non-Pathogenic Glomerulus	341	0	4	12	95.518	
	pred. non-Pathogenic Tubulus	3	243	0	0	98.780	
	pred. Pathogenic Glomerulus	26	0	318	11	89.577	
	pred. Pathogenic Tubulus	27	5	16	315	86.777	
	class recall	**85.894**	**97.984**	**94.083**	**93.195**		**92.127**

B. Salient Object Detection

In the specific images four (4) types/classes of salient objects are recognized. They are namely: non-Pathogenic Glomerulus, Pathogenic Glomerulus, non-Pathogenic Tubulus and Pathogenic Tubulus. Non-pathogenic and pathogenic Glomerulus has a diameter ranging from 50 to 120 μm [12]. The tubules of the nephrons are 30 – 55 mm long [13] with an average diameter of 50μm.

Since the edges of the targeted regions are not clear in the biopsy images, a block based segmentation approach is adopted. The image is divided in blocks (squares). Segmentation squares are much smaller than the aforementioned objects. The size of the block is set 37x37. This value has been selected heuristically, as the most appropriate for providing satisfying accuracy and acceptable processing times, based on conducted experiments.

For the feature extraction procedure, customized code was developed in order to separate the ROI into smaller square segments of a specific width (defined by the user and 37x37 in our case). Mean, Standard deviation, Contrast, Inverse Difference Moment, Correlation, Entropy and Angular Second Moment are the features, which were used as inputs for the classification of each segmentation block. The above features have been selected as the most appropriate textural features for image classification [14]. The only preprocessing step of the image data concerns gray scale conversion. Some additional preprocessing techniques were tested (i.e. histogram equalization and contrast enhancement etc,) but they were omitted at the end, since they provided lower accuracy.

Each block is allocated through the classification procedure to a specific class. Four widely known classifiers were examined, namely: Support Vector Machines (SVM) [15], Naïve Bayes [16], K-Nearest Neighbor [17] and Decision trees [18].

During the training procedure of the classification model, representative regions were selected through the above feature extraction procedure. The expert biologists participating in this research did the selection. This resulted in a training set of about 1200 segmentation squares (400 of each class). The ten-fold cross validation [19] has been adopted as a method for testing the accuracy. As depicted in Table I, the results are satisfactory. The best performing classifier for the current problem is the SVM classifier achieving 94.7% accuracy according to ground truth blocks, defined by the experts.

The produced segmented images are quite noisy, thus a morphological filtering is required (see Fig. 3). A simple pixel majority vote [20] recursive technique with a dynamic vote limit proved sufficient for this task. Regarding the Glomerulus object, a threshold of a minimum area of 7 blocks is set because as it noticed through experiments and observation, there is no glomerulus smaller than 9 blocks. The whole segmentation procedure is depicted in Fig. 4 for several images.

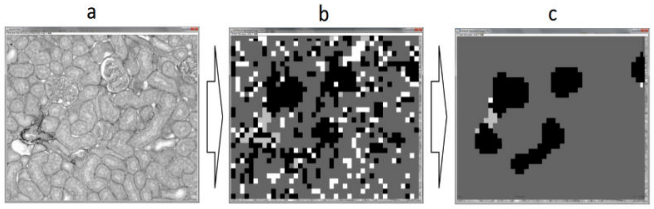

Figure 3. a) Original image, b) Segmented image, c) Majority vote enhanced

C. Image Characterization

Through the classification of the blocks and the assistance of majority vote technique, salient object detection is achieved. Following the image segmentation, features of the detected total regions may be calculated. The calculation of 23 features is supported by the developed application (Mean, Standard Deviation, Correlation, Angular Second Moment, Inverse Difference Moment, Contrast, Entropy, Minimum Grayscale value, Maximum Grayscale Value, Mode, ROI's height, ROI's width, ROI's percentage, Area (in pixels), Median, Kurtosis, Skewness, Histogram's minimum value, Histogram's maximum value, Area Fraction, Centroid, Angle and Center of Mass). The above set of features provides additional information about the characterization of a salient object.

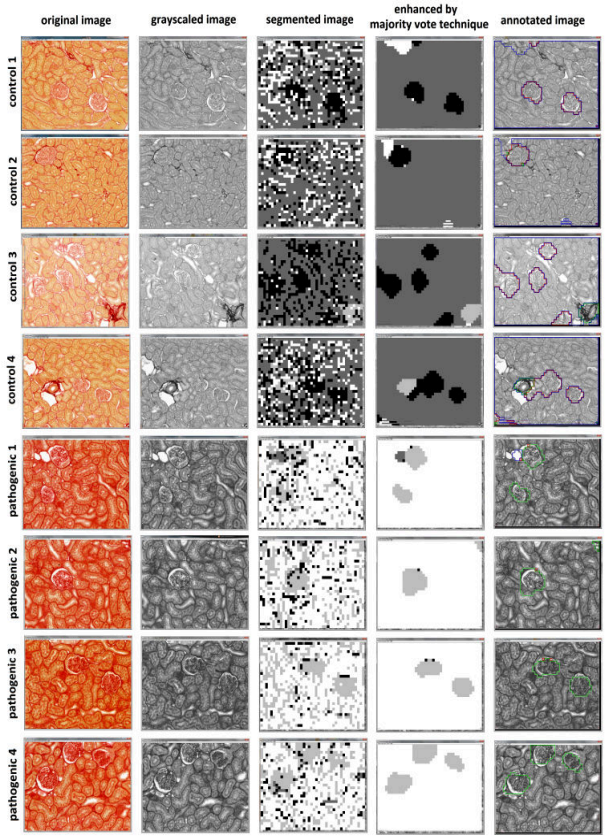

Figure 4. Automated Segmentation and Annotation Results

IV. Experimental Results

As it can be noticed in Fig. 4, the automated segmentation and characterization feature of the proposed application manages to detect the salient objects in the kidney biopsy images. The tool was tested in eight random (8) unknown images from the 60 images dataset, in order to prove its versatility: four (4) healthy/control and four (4) pathogenic. The corresponding results are presented in Table II, where Area Involved column stands for the percentage of the image that represents a specific salient foreground object.

The sensitivity, specificity and accuracy percentages of the tool are presented in Table III. As it can be noticed, since the background classes (Pathogenic Tubulus and Non-pathogenic Tubulus) cannot be count as a unit, the above values are presented only for the foreground objects. Some objects are miss–recognized with their corresponding opposite state object in control images (false positives). This occurs rarely, due to some similarities in textural features. Another miss-recognition cause is linked with the existence of artifact objects, which are not informative and put additional "noise" to the kidney biopsy images. Nevertheless

the performance is considered satisfying by the collaborating biologists and the achieved quantification quite useful for several images batch processing.

TABLE II. TEST OF THE IMPLEMENTED MODEL

Image ID	Number of Salient Objects	Description	Area Involved (%)	Current run's accuracy (%)
control1	2	Non-Pathogenic Glomerulus	3	100
		Non-Pathogenic Glomerulus	3	
control2	1	Non-Pathogenic Glomerulus	4	100
control3	5	Non-Pathogenic Glomerulus	2	80
		Non-Pathogenic Glomerulus	3	
		Non-Pathogenic Glomerulus	2	
		Non-Pathogenic Glomerulus	3	
		Pathogenic Glomerulus	4	
control4	2	Non-Pathogenic Glomerulus	8	100
		Non-Pathogenic Glomerulus	2	
pathogenic1	2	Pathogenic Glomerulus	4	100
		Pathogenic Glomerulus	2	
pathogenic2	2	Pathogenic Glomerulus	0	50
		Pathogenic Glomerulus	6	
pathogenic3	2	Pathogenic Glomerulus	4	100
		Pathogenic Glomerulus	3	
pathogenic4	3	Pathogenic Glomerulus	4	100
		Pathogenic Glomerulus	2	
		Pathogenic Glomerulus	4	

TABLE III. APPLICATION'S ACCURACY, SPECIFICITY AND SENSITIVITY

		Condition (as determined by "Ground Truth")		Predictive Values (%)
		Non-Pathogenic Glomerulus	Pathogenic Glomerulus	
Test Outcome	Non-Pathogenic Glomerulus	9	0	100
	Pathogenic Glomerulus	1	10	90.90909091
		90	100	95
		Sensitivity (%)	Specificity (%)	Total Accuracy (%)

V. CONCLUSION

In this paper we presented a novel tool for segmenting and characterizing microscopic kidney biopsies. The achieved accuracy results are quite satisfying. Although some misclassifications arise that should be treated in future work, the proposed methodology has been proved effective and useful for automated detection and quantification of pathogenesis in Kidney biopsy images.

ACKNOWLEDGMENT

This work was funded by EU ICT program "e-Laboratory for Interdisciplinary Collaborative Research in Data Mining and Data-Intensive Sciences (e-LICO)". Authors would also like to thank Joost Schanstra and Julie Klein from INSERM for the provision and annotation of the biopsy images.

REFERENCES

[1] S. Klahr, "Obstructive nephropathy". Department of Internal Medicine, Barnes-Jewish Hospital (North Campus) at Washington University School of Medicine, *Internal medicine* pp. 355-361, 2000.

[2] I. Maglogiannis, H. Sarimveis, C. Kiranoudis, A. Chatzioannou, N. Oikonomou, and V. Aidinis, "Radial Basis Function neural networks classification for the recognition of idiopathic pulmonary fibrosis in microscopic images", *IEEE Transactions on Information Technology in Biomedicine*, 12(1), pp. 42-54, 2008.

[3] T. Caballero, A. Pérez-Milena, M. Masseroli, F. O'Valle, F. J. Salmerón, R. M. G. Del Moral, and G. Sánchez-Salgado, "Liver fibrosis assessment with semiquantitative indexes and imageanalysis quantification in sustained-responder and non-responder," *Journal of Hepatology*, vol. 34, pp. 740-747, 2001.

[4] M. Masseroli, T. Caballero, F. O'Valle, R. M. G. Del Moral, A. Pérrez-Milena, and R. G. Del Moral, "Automatic quantification of liver fibrosis: design and validation of a new image analysis method. Comparison with semi-quantitative indexes of fibrosis", *Journal of Hepatology*, vol. 32, pp. 453-464, 2000.

[5] M. Yagura, S. Murai, H. Kojima, H. Tokita, H. Kamitsukasa, and H. Harada, "Changes of liver fibrosis in chronic hepatitis C patients with no response to interferon-α therapy: including quantitative assessment by a morphometric method", *Journal of Gastroenterology*, vol. 35, pp. 105-111, 2000.

[6] P. Bedossa, D. Dargere, and V. Paradis, "Sampling variability of liver fibrosis in chronic hepatitis C.," *Hepatology*, vol. 38 no. 6, pp. 1449-1457, 2003.

[7] M. A. Hussain, S. N. Merchant, L. S. Mombasawala, and R. R. Puniyani, "A decrease in effective diameter of rat mesenteric venules due to leukocyte margination after a bolus injection of pentoxifylline—digital image analysis of an intravital microscopic observation", *Microvascular Research*, vol. 67, pp. 237-244, 2004.

[8] K. Shiraishi, H. Takihara, and K. Naito, "Quantitative analysis of testicular interstitial fibrosis after vasectomy in humans," Aktuelle Urol., vol. 34 no. 4, pp. 262-264, 2003.

[9] K. Shiraishi, H. Takihara, and K. Naito, "Influence of interstitial fibrosis on spermatogenesis after vasectomy and vasovasostomy," *Contraception*, vol. 65 no. 3, pp. 245-249, 2002.

[10] G. Izbiki, M. J. Segel, T. G. Christensen, M. W. Conner, and B. R., "Time course of bleomycin-induced lung fibrosis," Int J. Exp. Path, vol. 83, pp. 111-119, 2002.

[11] P. König, C. Kayser, V. Bonin, and R. P. Würtz, "Efficient evaluation of serial sections by iterative Gabor matching", *Journal of Neuroscience Methods*, vol. 111, pp. 141–150, 2001.

[12] J.P Royet, C. Souchier, F. Jourdan, H. Ploye, "Morphometric Study of the Glomerular Population in the Mouse Olfactory Bulb: Numerical Density and Size Distribution Along the Rostrocaudal Axis", The journal of comparative neurology 270559-568 (1988)

[13] "Proximal convoluted tubule." *Encyclopædia Britannica. Encyclopædia Britannica Online*. Encyclopædia Britannica, 2011. Web.27Jun.2011http://www.britannica.com/EBchecked/topic/480781/proximal-convoluted-tubule.

[14] M. Haralick et al, (1973) Textural Features for Image Classification. IEEE Transactions on systems man and cybernetics Vol. SMC-3 pp. 610-621

[15] C. Cortes, V. Vapnik, "Support-Vector Networks", *Machine Learning*, 20, pp.273-297, 1995.

[16] Friedman N, Geiger D, Moises et al., "Bayesian Network Classifiers", *Machine Learning*, pp. 131-163, 1997.

[17] N. Roussopoulos, S. Kelley, F. Vincent, "Nearest Neighbor Queries", SIGMOD '95 Proceedings of the 1995 ACM SIGMOD international conference on Management of data ISBN:0-89791-731-6, p71-79, 1995.

[18] T. Mitchell, "Decision Tree Learning", in T. Mitchell, *Machine Learning,* The McGraw-Hill Companies, Inc., 1997, pp. 52-78

[19] R. Kohavi, "A Study of Cross-Validation and Bootstrap for Accuracy Estimation and Model Selection." *Proceedings of the 14th International Joint Conference on Artificial Intelligence* P.1137—1143, 1995.

[20] Balazs Harangi, Rashid Jalal Qureshi, Adrienne Csutak, Tünde Petö, András Hajdu. Automatic detection of the optic disc using majority voting in a collection of optic disc detectors. In Proceedings of ISBI'2010. pp.1329-1332

[21] C. Doukas, T. Goudas, S. Fischer, I. Mierswa, A. Chatziioannou and I. Maglogiannis, "An Open Data Mining Framework for the Analysis of Medical Images: Application on Obstructive Nephropathy Microscopy Images." *In: Proc. of the 32nd Annual International Conference of the IEEE Engineering in Medicine and Biology Society*, 2010, Buenos Aires, Argentina, 4108-4111.